IEEE Access
Multidisciplinary ⋮ Rapid Review ⋮ Open Access Journal

Received 3 January 2024, accepted 22 January 2024, date of publication 29 January 2024, date of current version 15 February 2024.

Digital Object Identifier 10.1109/ACCESS.2024.3359300

RESEARCH ARTICLE

A Novel Score-Based LiDAR Point Cloud Degradation Analysis Method

SEPEEDEH SHAHBEIGI[1,2], JONATHAN ROBINSON[2], AND VALENTINA DONZELLA[2]
[1]Department of Computer Science, University of York, Heslington, YO10 5DD York, U.K.
[2]WMG, The University of Warwick, CV4 7AL Coventry, U.K.

Corresponding author: Sepeedeh Shahbeigi (sepeedeh.shahbeigi@york.ac.uk)

Co-funded by the European Union. Views and opinions expressed are however those of the author(s) only and do not necessarily reflect those of the European Union or European Climate, Infrastructure and Environment Executive Agency (CINEA). Neither the European Union nor the granting authority can be held responsible for them. Project grant no. 101069576. UK participants in this project are co-funded by Innovate UK under contract no.10045139; and in part by the Centre for Doctoral Training to Advance the Deployment of Future Mobility Technologies (CDT FMT) at The University of Warwick.

ABSTRACT Assisted and automated driving systems critically depend on high-quality sensor data to build accurate situational awareness. A key aspect of maintaining this quality is the ability to quantify the perception sensor degradation through detecting dissimilarities in sensor data. Amongst various perception sensors, LiDAR technology has gained traction, due to a significant reduction of its cost and the benefits of providing a detailed 3D understanding of the environment (point cloud). However, measuring the dissimilarity between LiDAR point clouds, especially in the context of data degradation due to noise factors, has been underexplored in the literature. A comprehensive point cloud dissimilarity score metric is essential for detecting severe sensor degradation, which could lead to hazardous events due to the compromised performance of perception tasks. Additionally, this score metric plays a central role in the use of virtual sensor models, where a thorough validation of sensor models is required for accuracy and reliability. To address this gap, this paper introduces a novel framework that evaluates point clouds dissimilarity based on high-level geometries. Contrasting with traditional methods like the computationally expensive Hausdorff metric which involves correspondence-search algorithms, our framework uses a tailored downsampling method to ensure efficiency. This is followed by condensing point clouds into shape signatures which results in efficient comparison. In addition to controlled simulations, our framework demonstrated repeatability, robustness, and consistency, in highly noisy real-world scenarios, surpassing traditional methods.

INDEX TERMS 3D point cloud, noise factor, perception and sensing, sensor degradation.

I. INTRODUCTION

Autonomous driving systems hold the promise of revolutionizing transportation by providing safer and more efficient mobility [1], [2]. Ensuring the safety and reliability of these systems is of paramount importance, and redundancy of data plays a crucial role in achieving this goal [3]. Recent advances in semiconductor technology have propelled LiDAR (Light Detection and Ranging) technology forward through miniaturization, integration of components, and providing higher processing power [4]. Thus this technology has emerged as a key component in Assisted and Automated Driving (AAD) systems [5]. LiDARs offer detailed high-resolution environmental information in the form of 3D point clouds. However, before adopting LiDAR technology extensively for perception tasks in AAD systems, it is crucial to develop a fundamental understanding of how varied environmental conditions can significantly impact the point clouds generated by LiDAR [6]. This understanding can be achieved through a thorough quantification of the effects that these conditions impose on the attributes and fidelity of point clouds.

A. POINT CLOUD COMPARISON

A method for point cloud comparison finds applications in diverse areas, including noise detection, sensor degradation

The associate editor coordinating the review of this manuscript and approving it for publication was Jie Gao.

assessment, and 3D model validation. Essential attributes for these methods are:

- **Rigid Body Transformation Invariance:** The comparison should not be affected by translation, rotation or scaling of the point cloud.
- **Robustness:** The comparison should be affected only by overall geometric properties of the point clouds. Small changes in the point clouds does not necessarily mean dissimilar point clouds. This is especially true in automotive applications.
- **Fairness:** The comparison process should adhere to fair evaluation criteria. For example, when assessing two point clouds gathered from the same scene using different LiDARs with varying resolutions, the method needs to recognize their shared scene identity. This becomes particularly critical when downsampling is necessary. In instances where point clouds, acquired from the same LiDAR but differing due to noise, undergo downsampling that fails to provide a high-quality representation, it may lead to inaccurate, high dissimilarity scores.
- **Efficiency:** The comparison method should be efficient, especially considering the large volume of point clouds.

In the field of AAD systems, LiDAR point cloud comparison has been predominantly used within the localization pipeline, through registration methods [7]. The underlying principle of registration method is to find point correspondences between point clouds of sequential captures. Some of the widely-used registration techniques are Iterative Closest Point (ICP) and Normal Distribution Transformation (NDT) [8], [9]. To improve the accuracy of registration (hence localisation) many variations of these correspondence-based methods has been proposed [10], [11], [12]. Besides point cloud registration methods, only a few other techniques, such as the Hausdorff or Chamfer distance methods, have been developed and are used in commercial software [13]. These techniques employ point-by-point correspondence search algorithms to identify the closest match in the target point cloud for each point in the reference point cloud [14]. Hausdorff and Chamfer distances have been developed for a more general comparison between point clouds, specifically, one prominent application is pattern recognition [15]. In pattern recognition, points from various objects surfaces are collected. If the geometrical distance between two sets of points (the distance denotes how dissimilar the two sets are) is within a specified range, the two sets can be assumed to representing the same object. For instance, these methods are used in classifying objects into pre-determined categories [16].

Moreover, recently Neural Network (NN) methods have been used in point cloud comparison either as part of a method or independently. Since NN can detect many features and objects in the scans, they are gaining popularity. However, the uncertainties associated with deep learning methods needs to be studied further to make them a practical solution for AAD applications, especially safety-critical systems [17]. A deep learning method that is frequently used for point cloud data analysis is PointNet [18]. PointNet takes a point cloud as an input and then outputs a feature vector which summarises the input point cloud and can later be used for comparison purposes using a distance metric. For example, PointNetLK uses sum of squared distances cost function to align point clouds [19]. Another NN method is called DeepPoint3D where local features of the point cloud are learned using a Convolutional-NN [20]. Similarly, these features can be compared for each point cloud. Measuring similarity between two point-clouds using NNs is still in early stages and needs to be validated further. Analysing these methods is beyond the scope of this paper.

Although the methods mentioned so far are effective in their specific tasks, they fail to achieve a comprehensive and universally applicable point cloud comparison metric to quantify different degrees of sensor degradation caused by environmental conditions [21], [22]. Additionally, point-by-point comparison of data used in these methods is highly sensitive to uncertainties and changes in the scene, making it difficult to distinguish environmental impacts from other scene changes. Another drawback of these techniques is their limited capacity to control the degree of change detection. Consequently, it remains unclear which elements of the scene exerted a more significant influence on the final comparison outcome. Moreover, due to the substantial size of point clouds, these methods tend to be computationally intensive. Furthermore, the output of these methods necessitates normalization to enable meaningful comparisons.

Several applications can benefit from a more comprehensive and adaptable point cloud comparison. For instance, comparing point clouds against reference data allows for evaluating sensor data quality, particularly in adverse weather conditions or other degradation events, with respect to AAD system safety requirements. Previous studies have highlighted the significant impact of degradation caused by poor weather conditions on perception algorithms [5], [6], [23]. Additionally, ensuring the safety of autonomous driving systems requires extensive testing, which is impractical through real-world driving alone. As a solution, a hybrid approach combining simulation and real-world experiments has to be adopted [24]. To validate the accuracy of simulation environments, sensor models, and degradation models against real-world conditions, a quantitative comparison method is indispensable. Moreover, assigning a value to each point cloud compared to a reference point cloud opens up the possibility of establishing a relationship between this score and various tasks in the AAD pipeline, such as the quality of object detection and decision-making.

B. CONTRIBUTIONS

To address existing shortcomings in point cloud comparison techniques, an innovative framework is introduced that delivers distinct and stable dissimilarity scores when comparing point cloud pairs. This framework aims to

robustly and efficiently evaluate dissimilarity in LiDAR point clouds across different environments. Our key contributions include:

- **Range-Based Downsampling**: Tailored to LiDAR data, this method retains critical information while assessing the overall spatial composition of point clouds.
- **Signature-Based Comparison**: Using Probability Density Functions (PDFs) as an example, this feature simplifies the task of comparison and adds resilience to changes in the environment, such as the presence of dynamic objects and occlusions.
- **Scale-of-Interest (SoI) Selection**: This feature allows users to specify a minimum SoI, enabling analyses tailored to application-specific requirements.
- **Elimination of Point-by-Point Comparison**: Unlike traditional methods that require correspondence detection, our approach streamlines the comparison process and significantly reduces computational time.

To validate the framework, both simulations and real-world LiDAR scans from various settings are used. In real-world experiments, despite our best efforts, slight changes in data collection and the environment are inevitable. To address this challenge, a statistical methodology that accounts for these variations, enhancing the framework's applicability and ensuring consistent comparison results is suggested. The proposed framework's performance is evaluated against benchmarks such as Hausdorff distance and ICP, confirming its efficiency, consistency, and computational advantages.

C. PAPER STRUCTURE

The structure of this study is outlined as follows: In Section II, a comprehensive review of existing methods employed in point cloud comparison is presented. Additionally, this section explores the details of two benchmark methods used in this work: 1- Iterative Closest Point (ICP), and 2- Hausdorff distance method. Moving on to Section III, various steps of the proposed method are described. This begins with an introduction to a novel range-based downsampling method, followed by an explanation of point cloud signatures and their comparison strategy. The subsequent section details the experimental setups for both simulated and real-world scenarios. In Section V, a thorough analysis is conducted, with a specific focus on rain-induced degradation, occlusion, and dynamic objects. This analysis draws from datasets obtained in both simulated and real-world situations. The article concludes with a succinct summary of key findings and potential directions for future research.

II. RELATED WORK

In this section, an overview of key methods for comparing point clouds is provided. Among these, two correspondence-based methods, namely ICP and Hausdorff distance, are examined in more detail and are employed as benchmarks for evaluating the hereby proposed point cloud comparison framework. Additionally, shape-distribution-based methods are reviewed as well. These methods, primarily employed for comparing 3D shapes, have served as partial inspiration for the proposed framework.

A. CORRESPONDENCE-BASED METHODS

Point cloud registration is a well-known shape/scan matching problem in computer vision and robotics. It aims to identify the rigid transformation between two or more point clouds by establishing correspondences between similar points within those clouds.

1) ITERATIVE CLOSEST POINT (ICP) ALGORITHMS

One common approach to point cloud registration is to detect a set of entities, such as points or features, in both point clouds and then use iterative methods to find the transformation that aligns the two point clouds based on these correspondences. The Iterative Closest Point (ICP) algorithm is a popular method that uses the Euclidean distance between the points in one point cloud and their correspondences in the other point cloud by minimizing a cost function [8], [10]. In other words, ICP seeks to find the best possible match between the two point clouds by adjusting their relative positions, making them align as closely as possible. This iterative refinement process continues until the algorithm converges to an optimal alignment, improving the overall alignment accuracy between the point clouds. Other methods, such as Generalized-ICP and Trimmed ICP, have been proposed to make the process more robust to incorrect correspondences and outliers [11], [12]. The Normal Distributions Transform (NDT) algorithm uses probabilistic methods to fit normal PDFs on points falling in cubic volumes of the point cloud. The transformation between two point clouds is estimated by associating the PDFs of these two point clouds [9].

For comprehensiveness the ICP algorithm with Root Mean Squared Error (RMSE) cost function is further expanded here as it is used as a comparison for the proposed metrics.The basic steps of ICP are briefly summarised in Fig. 1. The method has been mainly used for localisation applications, therefore it is usually performed to compare a moving point cloud, $\mathbf{Q}$, to a reference fixed point cloud, $\mathbf{P}$. The algorithm starts with an initial estimate of transformation matrix consisting of rotation and translation elements and applies it to points in $\mathbf{Q}$. Then the RMSE (which uses Euclidean distances) of corresponding points is calculated. This process is repeated until either a minimum target RMSE is achieved or number of iterations pass a certain user-defined value. Both these limits are assigned by user and depend on the specific application.

2) OTHER METHODS

While correspondence-based methods can provide good results to compare point clouds from the same scene, they are computationally expensive and heavily rely on the quality and correspondence of detected entities. Therefore, there is a need for more generic and more efficient methods to measure the similarity or dissimilarity between two point clouds.

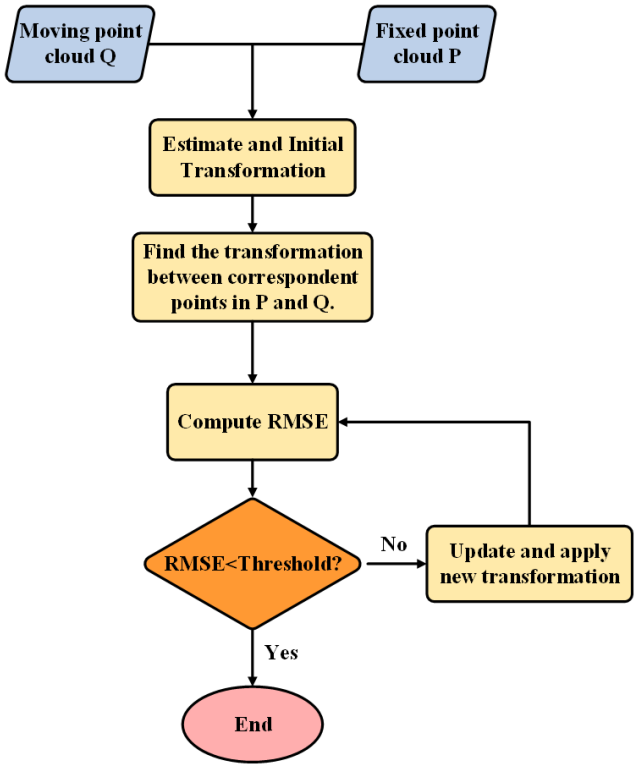

FIGURE 1. Flowchart of a standard Iterative Closest Point (ICP) algorithm to compare point cloud 'P' and 'Q' with RMSE as the cost function. RMSE threshold or maximum number of iterations are user defined.

A different type of correspondence-based methods that have been developed specifically for point cloud comparison are Hausdorff and Chamfer distances, which are still used in point cloud processing commercial software such as CloudCompare [13]. The proposed framework in this work is compared to the Hausdorff distance, therefore this distance is briefly explained here. The Chamfer distance slightly differs from Hausdorff distance.

The Hausdorff distance measures the maximum distance (average distance in case of Chamfer distance) from each point in one set to its nearest point in the other set. In the context of comparing two point clouds **P** and **Q**, the Hausdorff distance is defined as follows [25]:

$$d_H(P, Q) = \max \left\{ \sup_{p_i \in P} \inf_{q_i \in Q} \|p_i - q_i\|, \sup_{q_i \in Q} \inf_{p_i \in P} \|p_i - q_i\| \right\} \tag{1}$$

where p_i and q_i are points belonging to point clouds P and Q, respectively. The main disadvantage of Hausdorff and ICP-RMSE is that their output measures are not bounded, making the comparison among various scenarios under different conditions challenging.

B. SHAPE-DISTRIBUTION METHODS

Shape distributions are statistical models that describe shapes (with any dimensions). They have been used to quantify similarity between two shapes in many applications such as pattern recognition in computer vision. An important aspect in representing shapes as distributions (e.g. histograms or probability distributions) is to choose a shape function that captures distinct signatures of the shape. These shape functions can be distances between two random points on the surface, angles or areas that any three random points on the surface make [15].

An advantage of using shape distributions to compare point clouds is that the arduous tasks of registering the point clouds, detecting and matching features or model fittings, are no longer necessary. Furthermore, a whole point cloud is now represented by a histogram which ensures faster and more efficient computational effort compared to point-by-point comparison methods. This method has been mostly used in computer graphics and biology applications but there have been a few works that have applied it to point clouds [26], [27].

III. METHODOLOGY

In this section, the fundamentals of the proposed point cloud comparison framework are discussed. The framework comprises of two key steps: (1)- point cloud range-based downsampling, (2)- describing the downsampled point cloud using Probability Density Functions, and (3)- comparing the PDFs to generate a dissimilarity score. Due to the selected metric this score is bounded between 0 and 1. Furthermore, various techniques have been utilized to ensure a fair comparison between the PDFs. The overview of the proposed framework is presented in Fig. 2. Each stage is explained in details in the rest of this section.

A. NOVEL RANGE-BASED DOWNSAMPLING METHOD

Acknowledging the computational and time-intensive nature of direct point cloud analysis, a range-based downsampling method is introduced as the first step in the framework. LiDAR points are generally more accurate and offer higher resolution in close proximity to the sensor. Therefore, in line with our objective of efficient and precise point cloud comparison, our downsampling strategy prioritises points based on their closeness to the LiDAR sensor. Specifically, a greater number of points near the sensor and fewer as the distance increases are collected. This approach not only optimises computational speed but also retains essential elements necessary for an effective comparison.

In applications involving AAD, the point clouds can be remarkably large, often comprising millions of points to represent a single snapshot of the vehicle's surroundings. To ensure manageable processing, downsampling becomes essential. This process entails the removal of a portion of points from the point clouds. Several downsampling techniques exist, such as random elimination and grid averaging filtering methods. Random elimination method removes points by a user-defined percentage, while grid averaging method divides the point cloud into small cubes and selects representative points from each cube. These

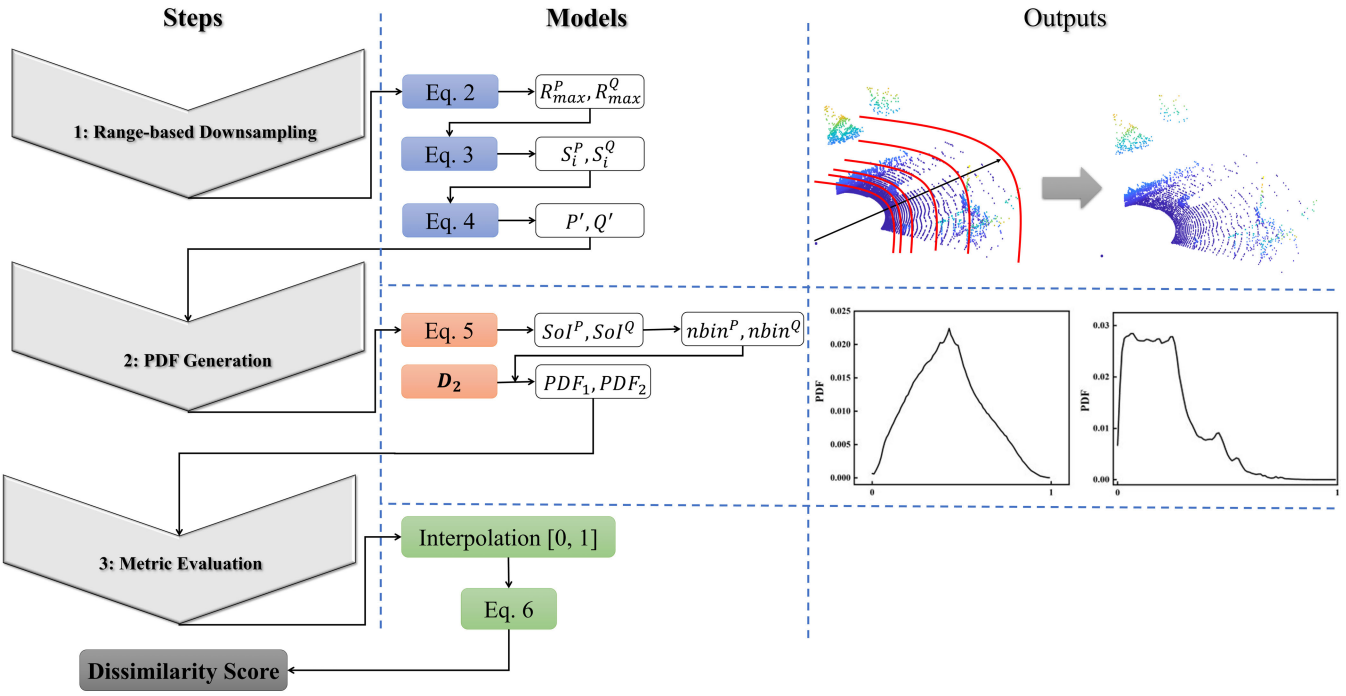

FIGURE 2. Steps of the proposed point cloud comparison framework, with relationship to equations and intermediate steps outputs.

methods do not take into account that the point cloud is denser near the LiDAR sensor and the accuracy per point is higher. The accuracy of the downsampled point cloud is crucial for effective point cloud comparison.

To address the shortcomings of traditional downsampling techniques, this paper introduces a novel range-based downsampling method. In order to maintain the critical features of the original point cloud, this method retains more points closer to the sensor and the number of retained points decreases as the distance from the sensor increases.

The method begins by identifying the maximum radial range in the point cloud P, denoted as $R_{\max}$ in Eq. 2, between the points in the point cloud p_i and the LiDAR sensor position $\bar{o}_L$:

$$R_{\max} = \max_{p_i \in \mathrm{P}} (\mathrm{d}(p_i,\ \bar{o}_L)) \tag{2}$$

In this equation, $\mathrm{d}(p_i,\ \bar{o}_L)$ is the Euclidean distance between p_i and $\bar{o}_L$. Subsequently, $R_{\max}$ is partitioned into n exponentially growing sections, each represented by Δr_i:

$$\Delta r_i = R_{\max} \times \left(1 - e^{-\lambda \cdot i}\right) \tag{3}$$

Here, λ is a parameter controlling the exponential growth rate. Within each section Δr_i, a uniform random distribution function is employed to sample a portion of the points, controlled by the user-specified parameter N:

$$P' = F\left(P_{S_i}, \frac{100}{N} \times |P_{S_i}|\right) \tag{4}$$

Fig. 3 illustrates a sample implementation of the range-based downsampling method. The maximum range is divided into 10 sections (Fig. 3a) and 25% of points in each section is selected. Due to this selection mechanism and the LiDAR data collection principle, the number of points in each section decreases as the distance from the sensor increases (Fig. 3c). This range-based approach provides a more selective method for capturing points from the scene compared to conventional random sampling techniques. This innovative range-based downsampling method facilitates the comparison of point clouds with different maximum ranges. Consequently, it enhances the robustness of comparisons, a crucial aspect for assessing the quality of point clouds, especially in ensuring the safety of AAD systems.

B. POINT CLOUD SIGNATURES AND COMPARISON

The second step of the proposed point cloud comparison framework starts with the calculation of a shape function on the point cloud. Next, a PDF from the shape function is created as a point cloud signature. Then, a suitable metric is used to compare the signatures of different point clouds effectively. The underlying concept involves condensing the intricate geometrical information characterizing the point cloud shape into a compact signature represented by a PDF. This PDF can be efficiently compared with other PDFs, enabling streamlined point cloud comparison. While this approach draws inspiration from pre-Neural-Networks era shape matching problems [15], it is tailored and refined to suit our LiDAR point cloud analysis to accommodate

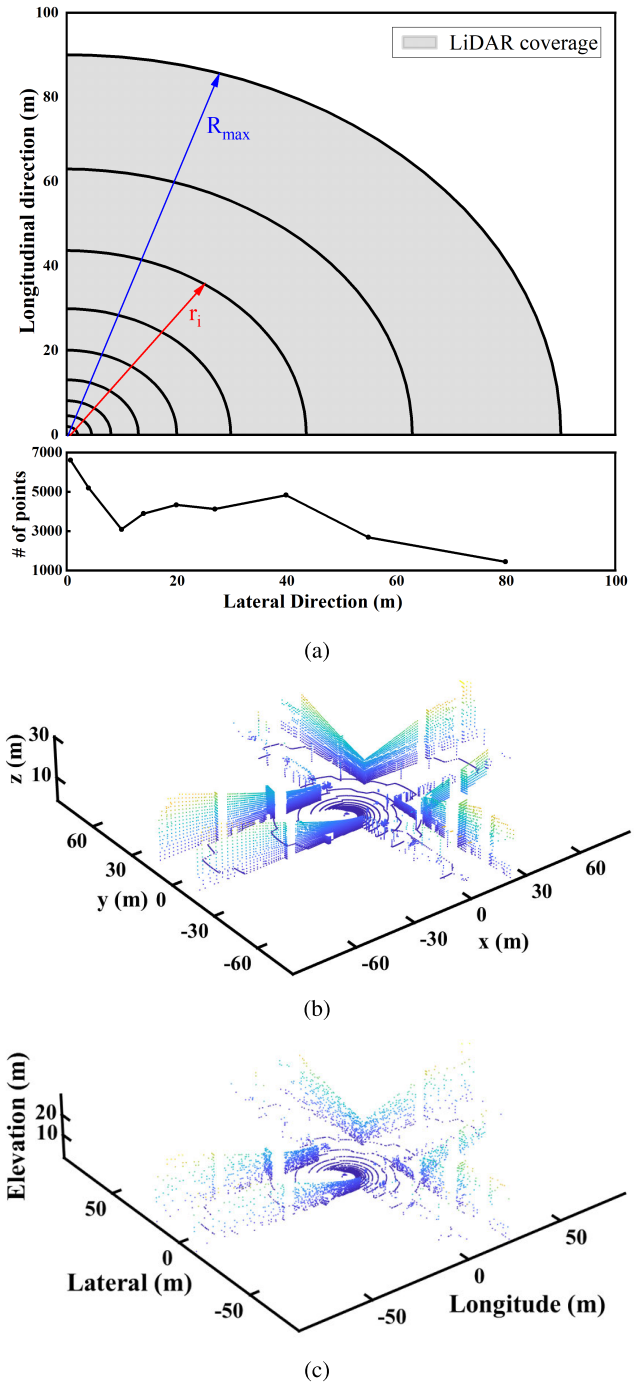

FIGURE 3. An example of the implementation of range-based downsampling method: a) schematic of range sections and number of points that fall in each section for a sample point cloud; b) the original point cloud; c) downsampled point cloud using range-based method with 10 sections and 25% of points in each section.

the fundamental characteristics that were defined in the introduction section:

- **Rigid Body Transformation Invariance:** The point cloud comparison framework ensures invariant comparisons by handling translations and rotations without the need for registration. It offers an efficient and robust solution for point cloud analysis, even in scenarios with less than 30% overlap between point clouds which results in unreliable results in registration methods.
- **Robustness:** To enable effective handling of small perturbations, occlusions, and dynamic objects within the scene. By comparing the point cloud signatures, the framework remains resilient to partial variations in the same scenes, making it advantageous for analyzing sensor degradation and validating sensor models.
- **Fairness:** Elements of the same scale are exclusively compared with one another in the two point clouds, providing an equitable and meaningful comparison.
- **Efficiency:** The proposed framework excels in efficiency compared to traditional point-by-point comparison methods (registration or Hausdorff methods). By summarizing the geometrical information into point cloud signatures, the comparison process becomes streamlined and efficient.

The foundational step in creating point cloud distribution signatures involves meticulously selecting geometric functions that generate unique distributions characterizing the point cloud shape. The proposed work focuses on surface attributes, including distances, angles, and areas, as they effectively represent the point cloud geometry. This study specifically employs **D2** function. This function calculates distances between every pair of points within the point cloud. The result is a square matrix, sized according to the point cloud, containing all pairwise distances. This matrix effectively captures the spatial relationships among the points in the point cloud.

In the next step, the PDFs are constructed based on the **D2** functions, representing essential geometric attributes of the point cloud. The determination of the number of bins for each PDF is directly influenced by the Scale of Interest (SoI), which represents the minimum scale of distance of interest in centimeters and is defined by user. The number of bins ($nbins$) based on SoI and maximum range (R_max) is defined by:

$$nbins = \lceil \frac{R_{max} \times 100}{SoI} \rceil \tag{5}$$

By adjusting the SoI, the PDFs are tailored to focus on desired specific geometric details.

While comparing two point clouds, the challenge arises when their PDFs have different numbers of bins and varying data ranges. To address this, an interpolation technique is adopted, mapping the PDFs onto a third PDF that spans the interval $[\min(\min(f_1), \min(f_2)), \max(\max(f_1), \max(f_2))]$ and separates it into n discrete intervals. This transformation ensures that the corresponding elements being compared in each bin align properly, allowing for an equitable comparison between the PDFs.

Now that the PDFs have been formed in a manner that ensures fairness in comparison, the next step is to select an appropriate metric for comparing them. The Hellinger

metric is selected for this matter, due to its following properties [14]:

- **Symmetry:** The Hellinger distance is symmetric, meaning $H(P, Q) = H(Q, P)$. Therefore, the order in which the PDFs are compared does not affect the result, ensuring fairness and consistency in the point cloud comparison process.
- **Sensitivity:** The Hellinger distance is sensitive to even small differences between PDFs, making it a reliable metric for detecting subtle variations in point cloud geometric signatures. This property is crucial for identifying sensor degradation and other critical changes in perception tasks.
- **Interpretability:** The Hellinger distance is interpretable, allowing researchers and practitioners to gain insights into the dissimilarity between point clouds based on the magnitude of the computed distance. A higher Hellinger distance indicates more significant differences between the PDFs and, consequently, between the corresponding point clouds.
- **Efficiency:** Computation of the Hellinger distance involves basic arithmetic operations, making it computationally efficient and suitable for large-scale point cloud comparisons, especially in the context of real-time applications in automated and autonomous driving systems.

The Hellinger distance is a metric widely used for comparing PDFs. Given two PDFs P and Q corresponding to different point clouds, the Hellinger distance $H(P, Q)$ is defined as follows:

$$H(P, Q) = \frac{1}{\sqrt{2}} \sqrt{\sum_{i=1}^{n} \left(\sqrt{p_i} - \sqrt{q_i}\right)^2}, \tag{6}$$

where p_i and q_i represent the probabilities at bin i for PDFs P and Q, respectively. The Hellinger distance ranges between 0 and 1, with 0 indicating that the two distributions are identical, and 1 indicating complete dissimilarity [14].

IV. GENERATION OF SIMULATION AND REAL-WORLD DATASETS

This section presents a comprehensive evaluation of the efficacy of the proposed point cloud comparison framework. The assessment involves subjecting the framework to various degradation levels using carefully controlled simulation data.

A. SIMULATION SETUP

In the simulation setup, the ego vehicle was equipped with a LiDAR sensor similar to the Velodyne Alpha Prime LiDAR, which closely replicates real-world LiDAR measurements. The LiDAR parameters are reported in Table 1. Both the simulation and the LiDAR sensor update at the same rate of 0.1 seconds (10 Hz) for simplicity.

The simulation spans a total duration of 126 seconds, allowing ample time to observe and evaluate the framework performance over an extended period. Throughout the simulation runs, the LiDAR sensor on the ego vehicle captures point cloud data at each time step, providing snapshots of the surrounding urban environment. Fig. 4 presents an example scene from the simulation, along with its corresponding LiDAR point cloud. To comprehensively study our proposed framework, variations of the simulation scenario are designed, namely: under rainfall conditions with various rain rates, occlusions, and dynamic object presence in the scene. These scenarios are detailed in following subsections.

TABLE 1. Velodyne Alpha prime LiDAR parameters.

Parameter	Value
Update Rate	10 Hz
Number of Channels	128
Vertical Field of View	40°
Vertical Resolution	0.2°
Horizontal Field of View	360°
Horizontal Resolution	0.1°
Maximum Range	180 meters

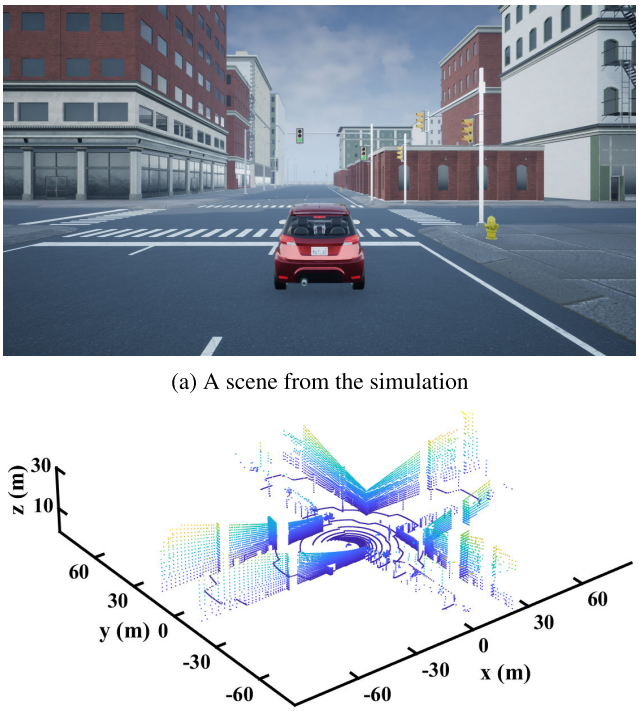

(a) A scene from the simulation

(b) LiDAR point cloud scan of the scene

FIGURE 4. An example of a simulated scene and its LiDAR point cloud scan generated by the virtual sensor.

1) RAINFALL CONDITION

In the context of sensor readings, adverse weather conditions such as rainfall can significantly impact data quality. To assess the robustness of the dissimilarity framework under rainfall-induced degradation, a well known rain model proposed is used [28], [29].

The model starts by considering range data, where it has been found that regardless of the rain rate (rr), the error on range measurements (d_i) remains below 2% [28]. To model rain noise on range, a sample is drawn from a normal distribution, $\mathcal{N}$, with a mean of zero and a standard deviation determined by d_i and R:

$$d_i' = d_i + \mathcal{N}(0, 0.02d_i(1 - e^{-rr})^2)) \tag{7}$$

Moreover, considering the impact of rain on point intensities (I_i), a fractional reduction parameter δ_i is introduced, representing the extent of intensity reduction for each point. This parameter is determined by the new range $d'i$ and the rain rate rr:

$$\delta_i = \frac{I_i - I_{i0}}{I_0} = e^{-2arr^b d_i'} - 1 \tag{8}$$

In this equation, I_{i0} represents the new intensity value for point i, and a and b are fitting parameters set to 0.01 and 0.6, respectively [29].

To account for significant signal attenuation that may lead to miss-detection of points, the new intensities I_i are further compared to the minimum detection threshold set by the LiDAR manufacturer, denoted as I_{min}. This threshold serves as a critical parameter to identify points with intensity values below the detectable range. The comprehensive process of this rain model, encompassing both range-based modifications and intensity reduction, is depicted in Fig. 5.

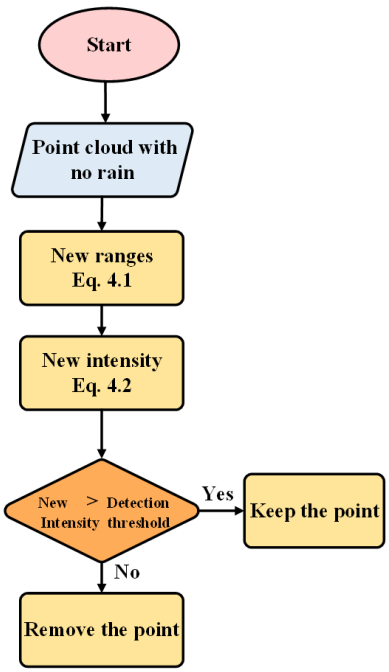

FIGURE 5. Flowchart depicting the implementation of the rain model on LiDAR point cloud data. The model simulates the effects of rain, including range data modification and intensity reduction.

2) OCCLUSION SCENARIO

The proposed Point Cloud Comparison Framework's strength lies in its utilization of PDFs as signatures, which suggests that the dissimilarity score will exhibit tolerance to occlusions and dynamic objects. To thoroughly investigate the impact of occlusions, a comprehensive study is conducted using scenarios involving multiple vehicles within the LiDAR's field of view (FoV), as illustrated in Figure 6.

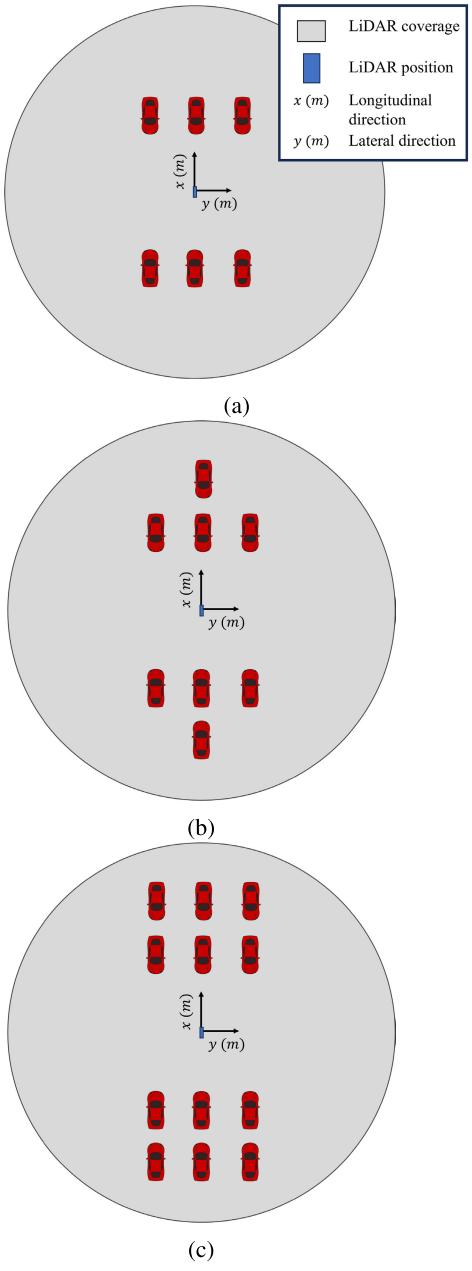

FIGURE 6. Occlusion scenarios: (a) 6 cars in the field of view without interfering with each other's points, (b) 8 cars with 2 of them out of the line of sight of LiDAR, and (c) 12 cars with 6 of them out of the line of sight.

In the scenarios, vehicles were strategically positioned to ensure that LiDAR beams hitting them do not interfere with each other, allowing for an isolated analysis of occlusion effects. To further evaluate the influence of occlusion, additional vehicles were placed behind the initial setup, resulting

in scenarios with eight and twelve vehicles (Figures 6b and 6c, respectively).

3) DYNAMIC OBJECTS

In addition to examining occlusions, our investigation also explores the influence of dynamic objects on the framework's performance. To conduct this assessment, four vehicles and two bicycles are introduced, strategically positioned with predefined initial locations and moving at constant velocities, as depicted in Figure 7. By incorporating dynamic objects into the scene, the aim is to thoroughly evaluate how the framework handles complex scenarios with moving elements. The presence of dynamic objects, such as other vehicles, pedestrians, and cyclists, in the operational environment of Autonomous and Automated Driving systems is inevitable. Therefore, it is crucial to analyse the performance of the proposed framework in the presence of such objects.

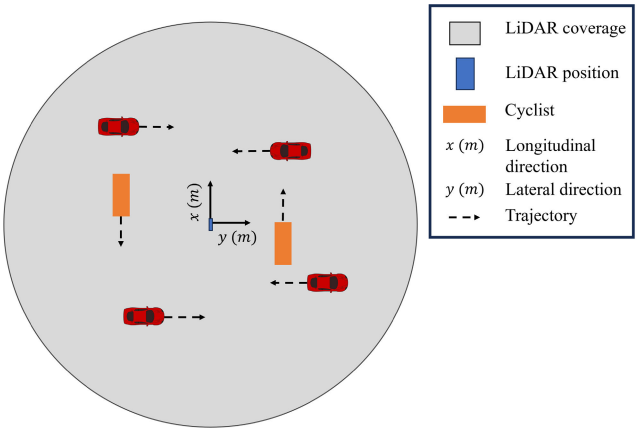

FIGURE 7. The scenario with dynamic objects. The scene includes four vehicles and two cyclists, all moving at constant velocities with various directions.

B. REAL-WORLD EXPERIMENT

Real world data was collected at the Carissma Outdoor Test Facility at the Technical University Ingolstadt of Applied Sciences in Germany, as part of the EU ROADVIEW project. The facility is an outdoor enclosed test track; therefore, provides a controlled environment to perform precise tests. The LiDAR used was an Ouster OS1 128 channel 360° LiDAR. Water sprinklers were set up along the test facility which when turned on were designed to create rainy conditions. There were 16 sprinklers in total, 8 on each side with 16m separation between them in the longitudinal direction and 8m between them laterally, as shown in Fig. 8. Data was collected both with the sprinklers turned off, creating the clear weather condition, and with them turned on, creating the rainy condition. Rain rate was designed to be the equivalent of 10mm/h but was measured to have a mean of 8.68mm/h. A Euro NCAP Car target was placed 28m from the LiDAR sensor to enable comparison of the LiDAR's ability to detect a target. The clear weather and rainy data is compared and the results are discussed in Section V and shown in Fig. 8.

FIGURE 8. Carissma outdoor test facility.

V. SIMULATION AND EXPERIMENTAL EVALUATION

In this section, the results of the comparative analysis of the proposed point cloud comparison framework are presented. The simulation studies were designed to test the framework's robustness and accuracy under various scenarios with controlled conditions. On the other hand, the real-world study was conducted to evaluate the framework in a practical setting. A comparative analysis is also performed between the proposed framework and the Hausdorff distance and ICP-RMSE methods, widely used for point cloud processing. The results of these studies are presented and discussed in detail below.

A. SIMULATION STUDY

In a preliminary assessment, a comparative analysis is performed using simulated data from both clear and rainfall weather conditions. The results of the proposed framework are compared with two other widely used techniques: 1) Hausdorff distance, and 2) the Root Mean Square Error (RMSE) obtained from the Iterative Closest Point (ICP) registration between two point clouds. By Comparing our proposed framework with two current methods in the literature, it is possible to discuss the shortcomings of these prevalent methods and how are proposed framework addresses them. Furthermore, this will shed light on the possible future directions of the current research. Fig. 9 showcases three heatmaps, each corresponding to one of these methods, to compare five consecutive scans from clear weather (names starting with clear) to themselves and to their associated rain condition scans (names starting with rain). The calculations are conducted using a rain rate of 30 mm/hr.

An immediate advantage of our proposed framework is observed in Fig. 9a, where the dissimilarity scores are presented. Our method's output dissimilarity score is always bounded between 0 and 1, without any post processing

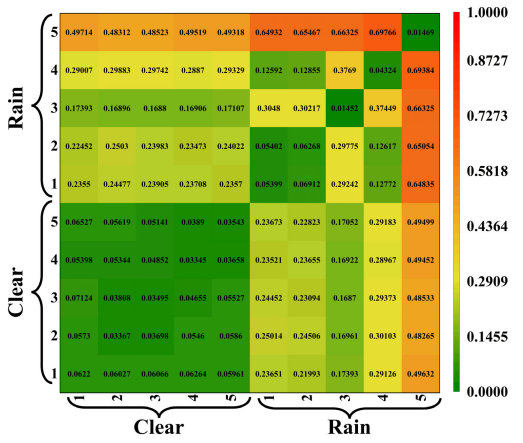

(a)

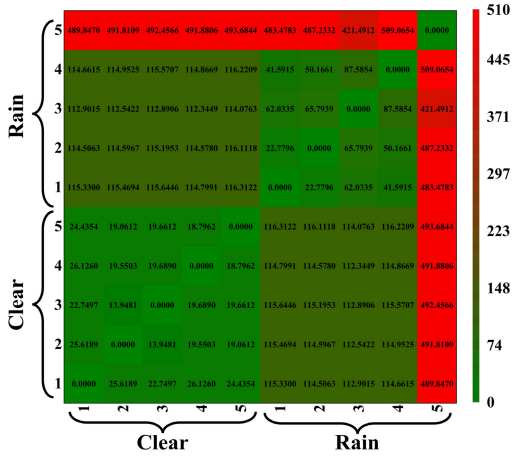

(b)

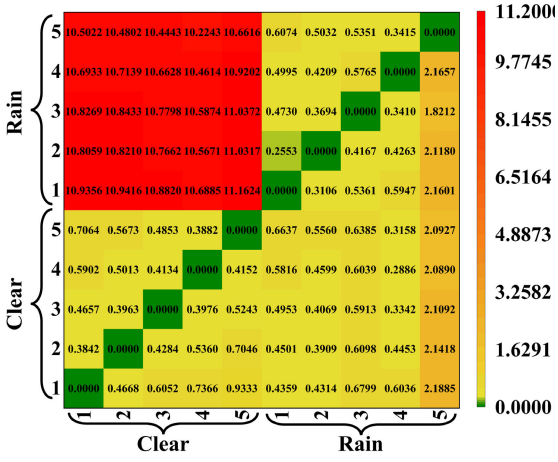

(c)

FIGURE 9. Comparing results of 50 consecutive clear weather scan from simulation and their associated rainy scans for: a) Our proposed framework. b)Hausdorff distance method, and c) ICP-registration's RMSE.

required. The scores calculated by the Hausdorff distance (Fig. 9b) and ICP-RMSE (Fig. 9c) are both unbounded; in other words, their output can take on any value up to infinity [14].

Another observation from Fig. 9a is that the score of comparing a scan with itself is not exactly zero due to randomness in the range-based downsampling unlike the Hausdorff distance and RMSE-ICP methods which both result in zero or very small values, respectively. However, the same-scan score from our framework represents the minimum value in the row. To minimize the impact of randomness, the percentage of points selected from each section was adjusted. Ultimately, 25% of points from 30 sections were selected, resulting in the minimum score value for the same-scan comparison.

Moreover, as scans are consecutive, an increase in the dissimilarity score is expected as they become further apart. Our proposed framework in Fig. 9a reflects this expected behaviour, in contrast to the Hausdorff distance (Fig. 9b) and ICP-RMSE (Fig. 9c) where the consistency seems somewhat random. For instance, in the last row of both Figs. 9b and 9c, the unbounded nature of the Hausdorff distance and ICP-RMSE methods makes interpreting the results challenging, especially in cases where different sensors with varying specifications are used.

Another essential advantage of our method is the ability to select a desired SoI. This flexibility allows us to either compare only the general large structures of two point clouds or focus on specific small effects, such as rain-induced degradation. In contrast, both the Hausdorff and ICP-RMSE are point-by-point comparison methods, and considering the uncertainties present in real-world data, the possibility of producing inconsistent result is high. This is clearly observed in Fig. 9b and Fig. 9c.

Furthermore, the ICP-RMSE is designed to register overlapping point clouds and slight changes in the environment, which are common in AAD applications, and may result in highly different scores. This sensitivity to minor variations poses challenges in real-world scenarios, where data can be subjected to clutter and dynamic objects in the scene. Moreover, the ICP-RMSE does not produce symmetric results (i.e. the results comparing point clouds P and Q is different from comparing Q and P) which is not desirable for point cloud comparison III-B. On the other hand, our proposed framework produces symmetric scores observed in Fig. 9a. In fact, symmetry is one of the motivations for selecting the Hellinger metric. While efforts have been made to select downsampling parameters that ensure repeatability of results, a certain degree of randomness persists. In our future work, we aim to refine the downsampling method to mitigate and eventually eliminate this remaining randomness. It is noteworthy that these small variations in the dissimilarity scores observed in Fig.9a is due to arithmetic rounding and this randomness.

Overall, according to results presented in Fig. 9, our proposed framework addresses limitations associated with conventional LiDAR point cloud comparison. The bounded dissimilarity score, the ability to set a desired SoI, and

the tolerance to environmental changes contribute to the versatility and effectiveness of our method for various applications in AAD systems. After highlighting the potential of our proposed framework to address drawbacks in conventional point cloud comparison methods through its ability to generate reliable and consistent results, the rest of this section will investigate other characteristics of our proposed framework.

B. SENSITIVITY ANALYSIS OF DENSITY CHANGE DETECTION

An evident consequence of degradation in LiDAR point clouds is the alteration in their density. For instance, when laser beams interact with raindrops, diffraction often occurs, resulting in a reduction of received signals below the detection threshold. As a consequence, the density of collected point clouds experiences a notable decrease compared to clear weather conditions [5].

This subsection focuses on investigating the sensitivity of our proposed point cloud comparison framework to density changes within the point clouds. To conduct a comprehensive examination of the effect of density change on dissimilarity, the analysis is confined solely to study changes in point cloud density.

To perform the analysis, 100 scans are selected from the simulation data, and a uniform random sampling method is employed to generate point clouds with densities ranging from 0.1 to 0.9 times that of the original. Each downsampled scan is then compared to its original scan. By systematically varying the densities while keeping other factors constant, the impact of density changes on the framework performance can be effectively observed and evaluated.

The objective of this investigation is to gain insights into how our framework responds to varying point cloud densities, providing valuable information for assessing its robustness and applicability across different density scenarios.

Figure 10 showcases the calculated scores resulting from the density analysis, which includes nine generated point clouds for each of the 100 total scans, leading to a total of 900 scans.

The analysis utilizes parameters determined in the preceding section, with the number of repetitions, radial sections, and percentage of points in each section set to 10, 30, and 25%, respectively. To avoid exceeding the number of points in the scan with a relative density of 0.1, a relatively larger Scale-of-Interest (SOI) of 30 centimeters is chosen. Furthermore, this ensures that the representative PDFs will not be sparsed which will result in inflated dissimilarity scores.

The results reveal a clear trend: as more points are selected, the average score decreases. This outcome aligns precisely with our expectations for this analysis: that when a larger number of points from both the original and generated point clouds overlap, a lower dissimilarity score is anticipated. However, due to the inherent randomness in the selection process, the dissimilarity score does not reach zero.

These findings provide valuable insights into how our proposed point cloud comparison framework responds to variations in point cloud density.

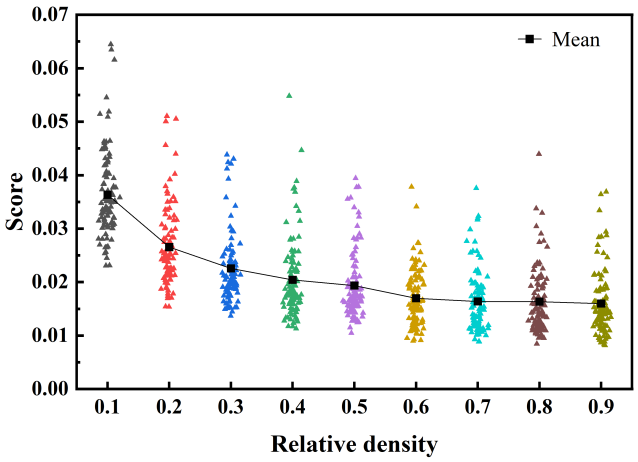

FIGURE 10. Analysis of point cloud density's impact on calculated scores. The generated point clouds have relative density of 0.1 to 0.9 times the original point cloud. The score is calculated by comparing each generated point cloud with its original one. The framework's parameters are from the previous section, with a Scale-of-Interest of 30 cms. The mean score decreases as the number of points in both point clouds become closer.

1) DEGRADATION LEVEL DETECTION

LiDAR point clouds are susceptible to noise, leading to disturbances and inaccuracies in the collected data. Factors such as atmospheric conditions, surface reflectance properties, and other interferences can contribute to noise, resulting in uncertainties within the point cloud data [5]. Motion artifacts, sensor imperfections, and hardware limitations can further exacerbate noise levels, affecting the accuracy of subsequent analyses.

In the study, varying rain intensities corresponding to different rain rates were simulated. Scans were collected from clear weather conditions, and various rainfall scenarios were applied. A comparative analysis was then performed by comparing each rain scan with its respective clear weather scan counterpart. The goal was to quantitatively assess the quality degradation caused by adverse weather conditions and evaluate the effectiveness of our Point Cloud Comparison Framework in identifying such scenarios.

Fig. 11 illustrates the dissimilarity scores averaged for the comparison of 20 scans in each rain rate condition. The examination of these scores demonstrates that our framework effectively quantifies the impact of rain-induced degradation on LiDAR point clouds. As the rain rate increases, the dissimilarity score also increases, indicating a higher level of dissimilarity between the point clouds. This finding aligns with expectations, as rain-induced noise and degradation pose challenges in accurately representing the scene.

These results have important implications for our framework applications. By quantifying the impact of rain on point cloud data, our framework can validate LiDAR rain

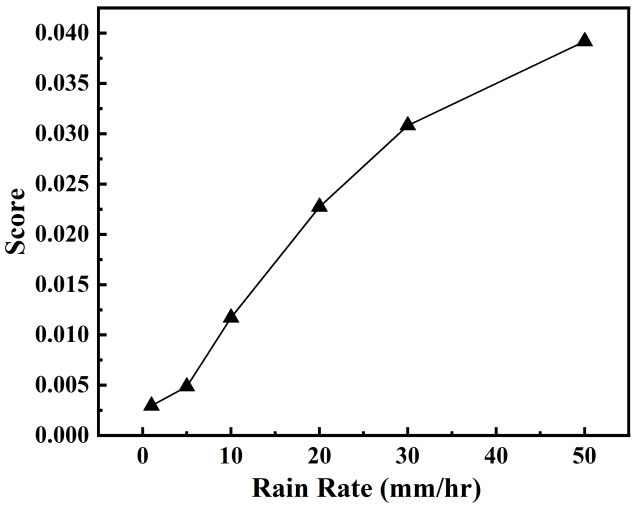

FIGURE 11. Effect of rainfall on dissimilarity scores: Higher rain rates results in increased dissimilarity between point clouds, showcasing the framework's ability to quantify rain-induced degradation.

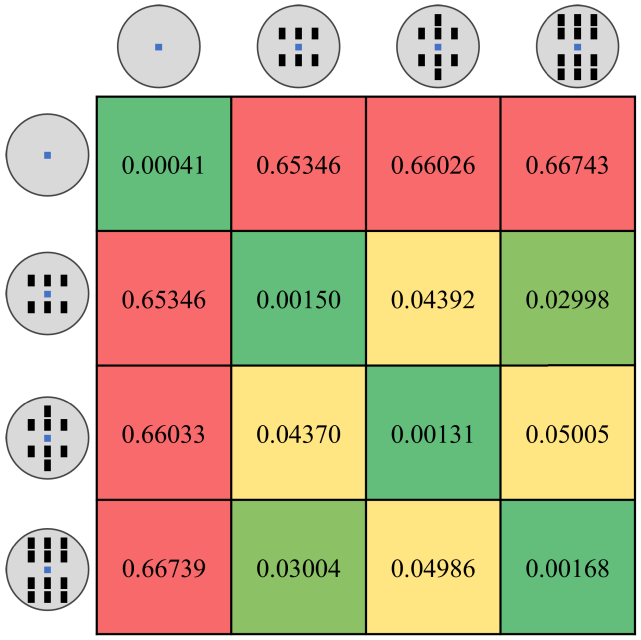

FIGURE 12. Heatmap of the dissimilarity score for various scenarios containing different number of vehicles in the scene. The occlusion from 12 cars scene, causes the similarity score to decrease.

models and assess their accuracy in replicating real-world scenarios. The ability to set a dissimilarity score threshold allows for the detection of significant deviations between clear weather and rain-induced scans, which is critical in safety-critical applications. The framework empowers researchers and engineers to make informed decisions regarding data quality and safety assessment in diverse weather conditions. For instance, in the heavy rain conditions the dissimilarity score demonstrates difference in the point clouds provided from the same scene. This information can be used to start a mitigation protocol to ensure the accuracy and safety of decisions that are made using these point clouds.

2) OBSTRUCTION AND DYNAMIC OBJECTS EFFECT

This subsection addresses the challenges faced by AAD systems, operating in diverse environments, including urban cities and small towns. The operational environment introduces complexities such as occlusions and the presence of dynamic objects within the scene. Our point cloud comparison framework exhibits a crucial advantage in handling such scenarios by leveraging the general geometric properties of point clouds, enabling it to tolerate obstructed views and moving elements effectively. This section focuses on comprehensively examining how these occurrences impact the outcomes of our framework.

The dissimilarity scores resulting from the occlusion effect are presented, using the range-based downsampling method with standardized and optimized parameters. Various scenarios were evaluated, comparing LiDAR point clouds under different conditions with different numbers of vehicles in the scene: No car, 6 cars, 8 cars, and 12 cars, as depicted in Fig. 6. The dissimilarity scores are illustrated in a heatmap (Fig. 12), with each row and column representing a scenario as depicted by the corresponding sketch.

Upon analyzing the dissimilarity score matrix, it is observed that the main diagonal elements (where the scenarios are compared to themselves) contain relatively low scores, as expected. This result validates the effectiveness of the range-based downsampling method in preserving the point cloud's structure when compared to itself.

The off-diagonal elements of the matrix reveal the dissimilarity scores between different scenarios. As anticipated, the dissimilarity scores increase as the number of occluding vehicles (e.g., "6Cars," "8Cars," and "12Cars") in the LiDAR point cloud's field of view increases. An interesting observation is the decrease of the dissimilarity score between 12Cars and 6Cars scenarios. This can be explained by considering the detection of the vehicles occluded by the ones closer to LiDAR. Therefore, as overall geometric properties of the point cloud in the form of a PDF are being analysed, these occlusions are ignored, resulting in a lower dissimilarity score.

For the evaluation of the proposed point cloud comparison framework under the presence of dynamic objects (as described in Section IV-A), the dissimilarity scores obtained from 10 scans were analysed. The mean dissimilarity score was found to be 0.23655, with a very low standard deviation of 0.000373 (Table 2). These closely clustered values indicate that our framework exhibits a high level of tolerance towards dynamic objects within the scene. The consistency of the dissimilarity scores suggests that the framework can effectively handle the presence of dynamic objects and maintain stable performance across multiple scans. The ability to obtain consistent and closely clustered dissimilarity scores showcases the robustness of our framework in assessing

point cloud comparison, even in scenarios where dynamic objects introduce temporal variations in the point cloud data.

TABLE 2. Scores for 10 scans in a scenario involving various dynamic objects with mean and standard deviation, σ.

#	Score
Scan 1	0.237365
Scan 2	0.236107
Scan 3	0.236385
Scan 4	0.236854
Scan 5	0.236457
Scan 6	0.236251
Scan 7	0.236745
Scan 8	0.236704
Scan 9	0.236355
Scan 10	0.236277
Mean	0.236550
σ	0.000373

C. REAL-WORLD EXPERIMENT

In this section, an illustrative example demonstrating the practical application of our point cloud comparison framework for quantifying and distinguishing between point clouds captured under diverse weather conditions is presented. Specifically, the framework effectiveness in assessing changes within the point cloud caused by rainy weather conditions, as described in Section IV-B, is showcased. Our dataset comprises of 326 dissimilarity scores obtained from repeated pairwise comparisons of 11 scans acquired in clear weather settings (clear-clear score), along with an additional 121 dissimilarity scores resulting from comparisons of 11 scans taken during rainy weather conditions relative to the reference scans in clear weather from the same scene (rain-clear scores). The rain intensity is at 10 mm/hr for the rainfall condition.

Furthermore, it is important to acknowledge that real-world LiDAR readings are subject to the influences of multiple factors, including ambient light, signal scattering, and absorption, leading to dissimilarity scores that differ even among scans captured in the same weather condition. Despite these intricate variables, our framework effectively demonstrates its ability to precisely quantify the degradation within point clouds. The probability distribution for the clear-clear and rain-clear scores are illustrated in Fig. 13a and Fig. 13b, respectively.

Since no clear recognizable or mutual distribution is seen in this data, and for inclusiveness, the permutation test was used. This non-parametric and robust method is employed in hypothesis testing for data with unknown distributions. The goal is to assess whether the dissimilarity scores derived from rain-clear comparison exhibit statistically significant differences from those of the clear-clear. Furthermore, by calculating a statistical threshold (critical value) with sufficient confidence, boundaries for clear weather and rainfall conditions (in this article only 10mm/hr rain condition) can

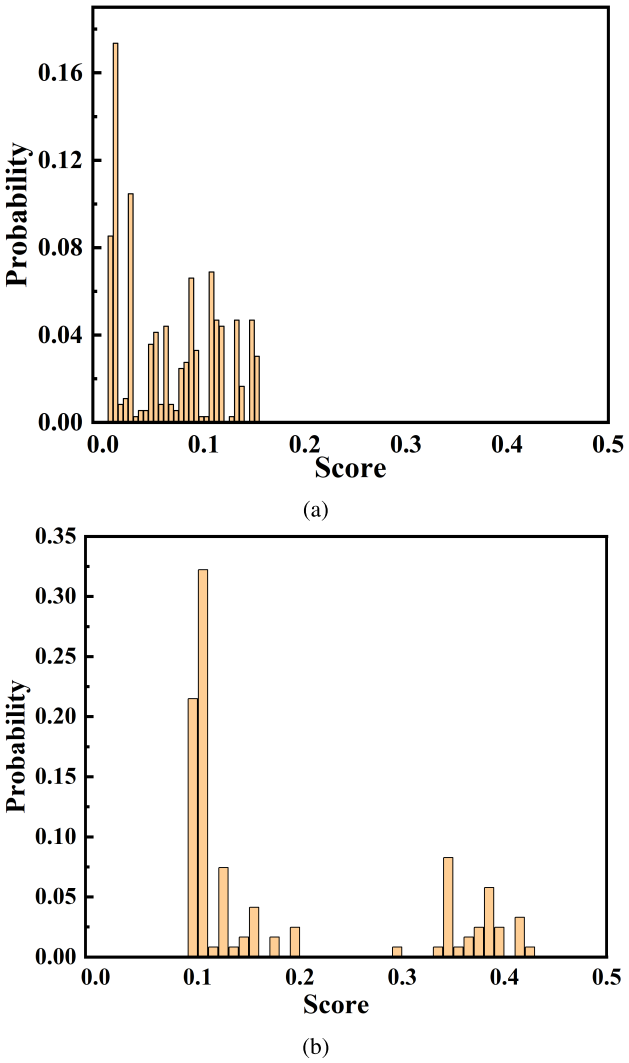

FIGURE 13. Probability distribution for a) 326 clear-clear scores and b) 121 rain-clear score.

be established. Formally, let X represent the dissimilarity scores for the rain-clear group, and Y denote the dissimilarity scores for the clear-clear group. The null hypothesis (H_0) and alternative hypothesis (H_1) are defined as:

$$H_0 : \text{No significant difference between two groups} \quad (9)$$

$$H_1 : \text{Significant difference between two groups} \quad (10)$$

In the context of hypothesis testing, the metric that describes the differences between two samples' parameters, used to reject or not reject H_0, is called test statistic. Here, the test statistic should adequately measure the difference in dissimilarity between the two sets of point clouds. In this study, the observed difference ($\delta_{\text{obs}} = mean(group1) - mean(group2)$) is calculated as the test statistic.

The core principle of permutation testing is shuffling the group labels (clear-clear and rain-clear groups) and recalculating the test statistic multiple times to create a distribution of test statistic values under the null hypothesis.

The permutation test procedure entails the following steps:

1) Compute the observed test statistic $\Delta\bar{x} = \bar{x}_X - \bar{x}_Y$, where $\bar{x}_X$ and $\bar{x}_Y$ are the means of the rain-clear and clear-clear groups, respectively.
2) Shuffle the group labels, randomly assigning the dissimilarity scores to new groups. Calculate the test statistic for each permutation, creating a distribution of test statistic values under random assignment.
3) Compare the observed test statistic $\Delta\bar{x}$ to the distribution of test statistic values generated from permutations. The p-value is calculated as the proportion of permutation test statistics that are more extreme than the observed test statistic. In other words, p-value represents the probability of observing a test statistic as extreme as the one computed from the actual data, assuming that the null hypothesis is true.

You can find the step-by-step process for hypothesis testing in Algorithm 1.

Algorithm 1 Permutation Test Algorithm

Require: n observations in group A, m observations in group B

Compute the observed test statistic T_{obs}
Initialize the number of permutations N_{perm}
Initialize an empty list to store permutation test statistics: $T_{\text{perm}} \leftarrow []$
for i from 1 to N_{perm} **do**
    Shuffle the observations in groups A and B randomly
    Compute the permutation test statistic T^i_{perm}
    Append T^i_{perm} to T_{perm}
end for
Compute the p-value as the proportion of T_{perm} values that are more extreme than T_{obs}:

$$p \leftarrow \frac{\text{count}\{T_{\text{perm}} > T_{\text{obs}}\}}{N_{\text{perm}}}$$

return p, T_{obs}

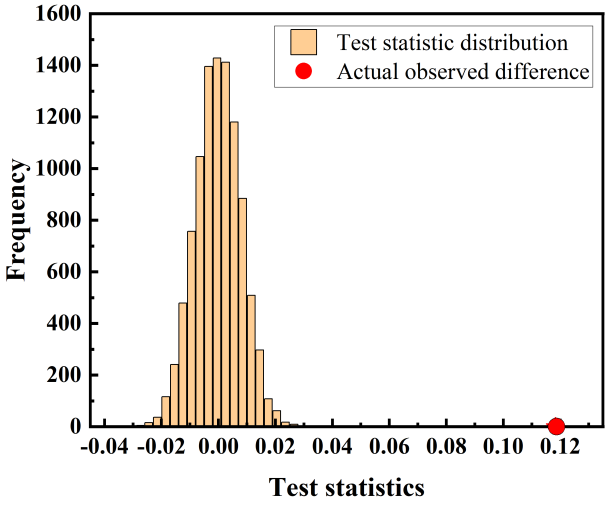

(a)

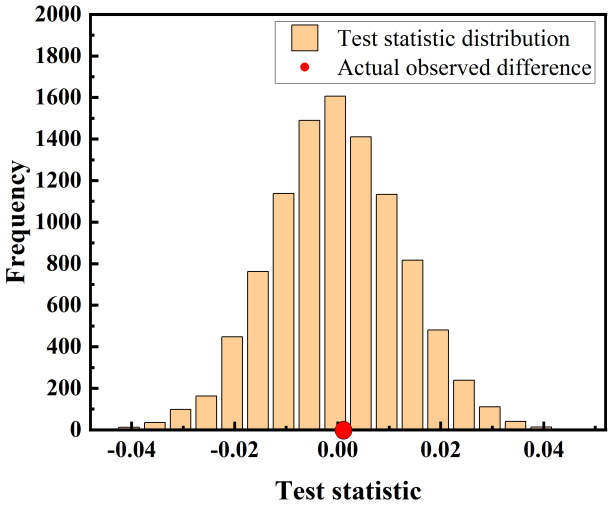

(b)

FIGURE 14. Permutation test results for a) clear-clear and rain-clear groups, and b) 50 new rain-clear and previous rain-clear group.

The observed difference in means $\Delta\bar{x}$ was 0.1182, resulting in a p-value of 0.0001 for 10000 permutations. The p-value is below the conventional significance level ($\alpha = 0.05$), allowing us to reject the null hypothesis. This outcome provides strong evidence that the dissimilarity scores effectively differentiate between rainy and clear weather conditions. The result of permutation test is illustrated in Fig. 14a.

Furthermore, an investigation was conducted to determine whether a subset of the rainy weather dissimilarity scores can be identified as belonging to the specific rain condition. A sample of 50 rainy weather scores was selected, and the permutation test was conducted for 10000 permutations. The observed difference in means was $-.0013$, resulting in a p-value of 0.5357. The p-value exceeded $\alpha = 0.05$, indicating that the subset of scores did not significantly differ from the complete rainy weather group. This finding showcases the framework's ability to recognize samples consistent with the specific rain condition with $10mm/hr$ intensity.

To sum up, our real-world experiment demonstrates the effectiveness and reliability of our proposed LiDAR point cloud comparison framework in identifying the impact of rain-induced degradation on point clouds. It has been attempted to apply ICP and Hausdorff in the real-word dataset, however due to their huge sizes, the current computational resource was insufficient. This also demonstrate the need for our proposed framework to ensure the efficiency of the point cloud comparison. Our future plan for this aspect involves conducting additional experiments with varying rain intensities and calculating dissimilarity score thresholds for each condition. This step can serve as a training phase. Then, these thresholds can be validated through testing using

more scans. Subsequently, these scores can be correlated with the results of other AAD systems (such as perception or decision-making modules) to assess the influence of sensor data quality on these tasks.

VI. CONCLUSION

In summary, the proposed Point Cloud Comparison Framework has proven to be a powerful and versatile tool for assessing the dissimilarity between LiDAR point clouds under various environmental conditions. The framework showed robust and interpretable performance, adequate for AAD applications, compared to the state-of-the-art point cloud comparison methods. Through extensive evaluation with simulation data and real-world scans, the framework exhibited robustness in handling occlusions, dynamic objects, and rain-induced noise. It's ability to generate bounded dissimilarity scores between 0 and 1 facilitates meaningful comparisons of point clouds from different scenarios, making it invaluable for safety-critical applications in autonomous driving systems.

As future work, the aim is to enhance the range-based downsampling method to minimize randomness and improve the consistency of dissimilarity scores. Achieving more reliable assessments will further strengthen the framework reliability. Additionally, our next step involves establishing the relationship between the calculated dissimilarity scores and their impact on perception tasks, such as object detection. Gaining insights into how degradations affect perception algorithms can contribute to enhancing the framework practical applications and furthering the advancement of autonomous driving technology. In conclusion, our Point Cloud Comparison Framework holds promise as a crucial tool in advancing LiDAR data analysis and perception tasks, with its robustness, interpretability, and applicability to real-world scenarios, making it a valuable asset in the pursuit of safe and reliable autonomous driving solutions.

REFERENCES

[1] E. Yurtsever, J. Lambert, A. Carballo, and K. Takeda, "A survey of autonomous driving: Common practices and emerging technologies," *IEEE Access*, vol. 8, pp. 58443–58469, 2020.

[2] D. Parekh, N. Poddar, A. Rajpurkar, M. Chahal, N. Kumar, G. P. Joshi, and W. Cho, "A review on autonomous vehicles: Progress, methods and challenges," *Electronics*, vol. 11, no. 14, p. 2162, Jul. 2022.

[3] M. Berk, O. Schubert, H.-M. Kroll, B. Buschardt, and D. Straub, "Exploiting redundancy for reliability analysis of sensor perception in automated driving vehicles," *IEEE Trans. Intell. Transp. Syst.*, vol. 21, no. 12, pp. 5073–5085, Dec. 2020.

[4] C.-P. Hsu, B. Li, B. Solano-Rivas, A. R. Gohil, P. H. Chan, A. D. Moore, and V. Donzella, "A review and perspective on optical phased array for automotive LiDAR," *IEEE J. Sel. Topics Quantum Electron.*, vol. 27, no. 1, pp. 1–16, Jan. 2021.

[5] J. P. Espineira, J. Robinson, J. Groenewald, P. H. Chan, and V. Donzella, "Realistic LiDAR with noise model for real-time testing of automated vehicles in a virtual environment," *IEEE Sensors J.*, vol. 21, no. 8, pp. 9919–9926, Apr. 2021.

[6] P. H. Chan, G. Dhadyalla, and V. Donzella, "A framework to analyze noise factors of automotive perception sensors," *IEEE Sensors Lett.*, vol. 4, no. 6, pp. 1–4, Jun. 2020.

[7] X. Huang, G. Mei, J. Zhang, and R. Abbas, "A comprehensive survey on point cloud registration," 2021, *arXiv:2103.02690*.

[8] X. Wang, Y. Li, Y. Peng, and S. Ying, "A coarse-to-fine generalized-ICP algorithm with trimmed strategy," *IEEE Access*, vol. 8, pp. 40692–40703, 2020.

[9] M. Magnusson, "The three-dimensional normal-distributions transform: Efficient representation for registration, surface analysis, and loop detection," M.S. thesis, Örebro Universitet, Örebro, Sweden, 2009.

[10] P. J. Besl and N. D. McKay, "A method for registration of 3-D shapes," *IEEE Trans. Pattern Anal. Mach. Intell.*, vol. 14, no. 2, pp. 239–256, Feb. 1992.

[11] A. Segal, D. Haehnel, and S. Thrun, "Generalized-ICP," *Robot. Sci. Syst.*, vol. 2, no. 4, p. 435, Jun.2009.

[12] D. Chetverikov, D. Stepanov, and P. Krsek, "Robust Euclidean alignment of 3D point sets: The trimmed iterative closest point algorithm," *Image Vis. Comput.*, vol. 23, no. 3, pp. 299–309, Mar. 2005.

[13] *Cloud-to-Cloud Distance*, 2015.

[14] M.-M. Deza and E. Deza, *Dictionary Distances*. Amsterdam, NL, Europe: Elsevier, 2006.

[15] R. Osada, T. Funkhouser, B. Chazelle, and D. Dobkin, "Shape distributions," *ACM Trans. Graph.*, vol. 21, no. 4, pp. 807–832, 2002.

[16] A. Javaheri, C. Brites, F. Pereira, and J. Ascenso, "A generalized Hausdorff distance based quality metric for point cloud geometry," in *Proc. 12th Int. Conf. Quality Multimedia Exper. (QoMEX)*, May 2020, pp. 1–6.

[17] R. L. Russell and C. Reale, "Multivariate uncertainty in deep learning," *IEEE Trans. Neural Netw. Learn. Syst.*, vol. 33, no. 12, pp. 7937–7943, Dec. 2022.

[18] R. Q. Charles, H. Su, M. Kaichun, and L. J. Guibas, "PointNet: Deep learning on point sets for 3D classification and segmentation," in *Proc. IEEE Conf. Comput. Vis. Pattern Recognit. (CVPR)*, Jul. 2017, pp. 77–85.

[19] Y. Aoki, H. Goforth, R. A. Srivatsan, and S. Lucey, "PointNetLK: Robust & efficient point cloud registration using PointNet," in *Proc. IEEE/CVF Conf. Comput. Vis. Pattern Recognit. (CVPR)*, Jun. 2019, pp. 7156–7165.

[20] S. Srivastava and B. Lall, "DeepPoint3D: Learning discriminative local descriptors using deep metric learning on 3D point clouds," *Pattern Recognit. Lett.*, vol. 127, pp. 27–36, Nov. 2019.

[21] A. Filgueira, H. González-Jorge, S. Lagüela, L. Díaz-Vilariño, and P. Arias, "Quantifying the influence of rain in LiDAR performance," *Measurement*, vol. 95, pp. 143–148, Jan. 2017.

[22] C. Zhang, Z. Huang, M. H. Ang, and D. Rus, "LiDAR degradation quantification for autonomous driving in rain," in *Proc. IEEE/RSJ Int. Conf. Intell. Robots Syst. (IROS)*, Sep. 2021, pp. 3458–3464.

[23] B. Li, P. H. Chan, G. Baris, M. D. Higgins, and V. Donzella, "Analysis of automotive camera sensor noise factors and impact on object detection," *IEEE Sensors J.*, vol. 22, no. 22, pp. 22210–22219, Nov. 2022.

[24] R. Donà and B. Ciuffo, "Virtual testing of automated driving systems. A survey on validation methods," *IEEE Access*, vol. 10, pp. 24349–24367, 2022.

[25] E. Deza and M.-M. Deza, *Dictionary Distances*. Amsterdam, NL, Europe: Elsevier, 2006.

[26] M. Mahmoudi and G. Sapiro, "Three-dimensional point cloud recognition via distributions of geometric distances," *Graph. Models*, vol. 71, no. 1, pp. 22–31, Jan. 2009.

[27] A. Wallace, S. Khastgir, X. Zhang, S. Brewerton, B. Anctil, P. Burns, D. Charlebois, and P. Jennings, "Validating simulation environments for automated driving systems using 3D object comparison metric," in *Proc. IEEE Intell. Vehicles Symp. (IV)*, Jun. 2022, pp. 860–866.

[28] C. Dannheim, C. Icking, M. Mäder, and P. Sallis, "Weather detection in vehicles by means of camera and LiDAR systems," in *Proc. 6th Int. Conf. Comput. Intell. Commun. Syst. Netw.*, May 2014, pp. 186–191.

[29] C. Goodin, D. Carruth, M. Doude, and C. Hudson, "Predicting the influence of rain on LiDAR in ADAS," *Electronics*, vol. 8, no. 1, p. 89, Jan. 2019.

SEPEEDEH SHAHBEIGI is currently pursuing the Ph.D. degree with the Intelligent Vehicle Directorate, WMG, The University of Warwick. She was with the Sensors Team, Intelligent Vehicle Directorate, WMG, The University of Warwick, to develop methods to ensure the reliability of sensor data, a pivotal aspect in the advancement of autonomous vehicle technologies. She is a Research Associate with the Assuring Autonomy International Programme (AAIP), Department of Computer Science, University of York. She has hands-on experience with advanced sensors, such as LiDAR and radar. She has contributed to projects on remote monitoring and supervision of autonomous vehicles. Additionally, she has experience working as a Graduate Teaching Assistant.

JONATHAN ROBINSON received the B.Sc. degree in mathematics and the M.Sc. degree in smart, connected, and autonomous vehicles from The University of Warwick, in 2018 and 2019, respectively. He has been with WMG, since 2019, in topics related to intelligent vehicles. He is currently a Project Engineer with the Intelligent Vehicles Sensors Group, WMG, The University of Warwick. His main research interests include perception sensors, simulation and modeling, and human factors. He has worked on a number of projects within these areas. The majority of his work focuses on LiDAR sensors and looking at noise, such as adverse weather and mutual interference.

VALENTINA DONZELLA received the B.Sc. degree in electronics engineering from the University of Pisa, Pisa, Italy, in 2003, and the M.Sc. degree in electronics engineering and the Ph.D. degree in innovative technologies for information, communication, and perception engineering from the Sant'Anna School of Advanced Studies, Pisa, in 2005 and 2010, respectively.

In 2009, she was a Visiting Graduate Student with the Engineering Physics Department, McMaster University, Hamilton, ON, Canada. She was a MITACS and a SiEPIC Postdoctoral Fellow with the Silicon Photonics Group, The University of British Columbia, Vancouver, BC, Canada. She is currently a Professor and the Head of the Sensors Area, Intelligent Vehicles Group, WMG, The University of Warwick, U.K. She is the first author, coauthor, and last author of several journal articles on top-tier optics and sensors journals. Her research interests include LiDAR, intelligent vehicles, integrated optical sensors, sensor fusion, and silicon photonics.

Prof. Donzella is a Full College Member of EPSRC and a Senior Fellow of the Higher Education Academy. She was awarded the Royal Academy of Engineering Industrial Fellowship on camera sensors.